International Journal of Heat and Mass Transfer 165 (2021) 120717

Contents lists available at ScienceDirect

International Journal of Heat and Mass Transfer

journal homepage: www.elsevier.com/locate/hmt

Convective heat transfer of nano-encapsulated phase change material suspension in a divergent minichannel heatsink

C.J. Ho [a,*], Yen-Chung Liu [a], Tien-Fu Yang [b,c], Mohammad Ghalambaz [d,e], Wei-Mon Yan [b,c,*]

[a] Department of Mechanical Engineering, National Cheng-Kung University, Tainan 70101, Taiwan
[b] Department of Energy and Refrigerating Air-Conditioning Engineering, National Taipei University of Technology, Taipei 10608, Taiwan
[c] Research Center of Energy Conservation for New Generation of Residential, Commercial, and Industrial Sectors, National Taipei University of Technology, Taipei 10608, Taiwan
[d] Metamaterials for Mechanical, Biomechanical and Multiphysical Applications Research Group, Ton Duc Thang University, Ho Chi Minh City, Vietnam
[e] Faculty of Applied Sciences, Ton Duc Thang University, Ho Chi Minh City, Vietnam

ARTICLE INFO

Article history:
Received 1 August 2020
Revised 15 October 2020
Accepted 2 November 2020
Available online 24 November 2020

Keywords:
Nano-encapsulated phase change materials
Water-NEPCM suspension
Divergent minichannel
Cooling performance

ABSTRACT

The convection heat transfer of nano-encapsulated phase change material (NEPCM)-water suspensions in a divergent minichannel heatsink was experimentally investigated. The mini heatsink was made of eight minichannels with a divergent angle of 1.38°. The minichannel was heated at the bottom, and the NEPCM-water was used as the cooling working fluid. The average Nusselt number, the index of performance, and the pressure drop of NEPCM-water compared to the pure water were examined. The experiments show that employing NEPCMs could be advantageous in low Reynolds number flows and low heating powers. The phase change heat transfer of NEPCM particles promoted the heat transfer by 82% compared to pure water. Moreover, using the NEPCM particles was not advantageous at large Reynolds numbers, where the sensible heat was the dominant mechanism of heat transfer.

1. Introduction

The advancement of technology in the miniaturization of electronic components and magnetic devices has increased the heat generation and surface heat fluxes of these elements. Moreover, PCMs can be used as an compact thermal energy storage medium [1,2]. In many cases, conventional heating techniques such as cooling by heatsinks or air cooling are not adequate. Hence, researchers continuously seek for practical approaches to address these technological cooling demands. Among the various proposed approaches, the microchannel and minichannel heatsinks have proven their high performance [3,4].

The heat transfer performance of micro/mini channels could be further improved by using an enhanced working fluid such as nanofluids [5,6] or hybrid nanofluids [7]. Many other approaches have also been reviewed in the study of Hussien et al. [8]. During the past several years, slurries of Micro-Encapsulated Phase Change Materials (MEPCMs) have been proposed and utilized as a potential type of working fluids. In MEPCM slurries, the microparticles could undergo a phase change and influence the heat transfer by phase change. The core of MEPCMs is made of a Phase Change Material (PCM), which melt/solidify at its fusion temperature and store/release heat to the surrounding in the form of latent heat. The PCM core is enclosed by a shell, which is typically a polymer. Recently, the MEPCM slurries and suspensions and their thermal and hydrodynamic properties have been reviewed in the comprehensive investigations of Delgado et al. [9] and Chen et al. [10].

Considering the application of MEPCM suspensions in channel heatsinks, Wang et al. [11] investigated the convective flow heat transfer of MEPCMs suspensions in a microchannel. The microchannel heatsink was a stainless-steel plate with ten carved microchannels of 0.35 × 0.35 mm cross-section and length of 440 mm. The microcapsules were made of paraffin-cores and melamine-formaldehyde resin shells, while the host fluid was water. The experimental results showed that using MEPCM-suspension could improve the Nusselt number by 1.36 times. Moreover, using the MEPCM particles could lead to a drastic increase of the pressure drop along the channel.

Sabbah et al. [12] theoretically examined the heat transfer and thermal performance of MEPCM-suspensions in a microchannel by a numerical 3D model. Their findings indicate that using MEPCM particles enhances the heat transfer and uniformity of the cooling. Still, the particular advantage of using encapsulated particles de-

* Corresponding authors.
E-mail addresses: cjho@mail.ncku.edu.tw (C.J. Ho), mohammad.ghalambaz@tdtu.edu.vn (M. Ghalambaz), wmyan@ntut.edu.tw (W.-M. Yan).

https://doi.org/10.1016/j.ijheatmasstransfer.2020.120717
0017-9310/

Nomenclatures

A_{ch}	the single-channel's cross-area at the inlet (m^2)
Ar	a single channel aspect ratio (H_{ch}/W_{ch})
COP	the coefficient of performance
C_p	the heat capacity per unit mass (J/(kg.K))
df	the measurement's uncertainty
D_H	the hydraulic diameter of the channel (mm)
f	the coefficient of the friction factor
FOM	the index of performance
H_c	the thickness of channel material at the thermocouple location (mm)
$\bar{h}$	the average of the forced convection heat transfer (W/(m^2 .K))
I	the supplied current to the element (A)
k	the thermal conductivity (W/(m . K))
L_{ch}	the channel length (m)
N	the number of the channels in the heatsink
$\overline{Nu}$	the average of Nusselt number in a channel
P	the consumed power for pumping working fluid through a channel (W)
p	the measured pressures (Pa)
Pe	Péclet number
q	cooling power (W)
q''	the element heat flux (W/m^2)
$\dot{Q}$	volumetric rate of the working fluid (m^3/s)
Re	Reynolds number
Sb	the subcooling number
Ste^*	the heating-power compared to the fusion's latent heat
T	the temperatures (°C)
T_M	the particle's fusion temperature (°C)
u_m	the average of the inlet velocity (m/s)
V	the supplied voltage to element (V)
W	the width of the channel (mm)
x_1, x_2, x_n	the experimental measurements

Greek symbols

β	the angle of channel pathway expansion (deg)
Δ	the difference operator
ΔH	the fusion's latent heat (J/kg)
ΔT_{ref}	a reference temperature $q_h/\rho_{bf}C_p\dot{Q}$ (°C)
Δx	an observation uncertainty
ε	the convection ratio
θ	the dimensionless temperature
μ	the working fluid's dynamic viscosity ($N.s/m^2$)
ρ	the working fluid's density (kg/m^3)
ω_{nepcm}	the nanoparticle's volumetric concentration (%)
ω_{pcm}	the nanoparticle's mass concentration (%)

Subscripts

bf	the host liquid
ch	the channel
eff	effective values based on the average of outlet and inlet
in	the inlet of a channel
m	an average property
mtd	computed values based on the average of outlet and inlet
$nepcm$	the nanocapsules
out	the outlet of a channel
tc	thermocouples
w	the channel's bottom wall

pends on the heating-power and the inlet cooling temperature as well as the fusion temperature of the particles. Liu et al. [13], utilizing a comprehensive model, analyzed the heat transfer behavior of MEPCM slurries in a rectangular microchannel. In their model, they considered the heat transfer resistance between the microparticles and the base fluid. Their findings showed that the Nusselt number could be raised to 190% by using 20% a mass fraction of microcapsules. They also reported that a channel with a larger aspect ratio (width/height) at its cross-section could better improve the releasing the latent heat of microparticles and the heat transfer.

In 2012, Farid and Al-Hallaj [14] filed a patent on the microchannel heat exchangers with MEPCM materials for cooling applications. In 2014, Wang [15] introduced a patent on the application of MEPCM liquids for cooling of automobile batteries. Ho et al. [16] experimented on the advantage of using divergent channels design in mini channel heatsinks. The results revealed that a divergent minichannel could improve the heat transfer rate and reduce the pressure drop. Thus, a divergent channel, which works with water as the coolant, provides a better coefficient of performance and lower thermal resistance compared to a parallel channel. Following [16], Ho et al. [17] examined the convective heat transfer and pressure drop of n-eicosane MEPCM-suspensions in divergent minichannel heatsinks. They examined the thermal performance of the suspension for two divergent angles of 1.36° and 2.06° and compared their findings with a parallel channel. They discovered that using MEPCMs improves heat transfer with the cost of a surge in the pressure drop. A divergent channel with an angle of 1.36° resulted in the improvement of the heat transfer and reduction of the pressure-drop penalty compared to a parallel channel. The improvement was pronounced at high Reynolds numbers and large concentrations of microparticles. Increasing the channel angle to 2.06° reduced the heat transfer at high Reynolds number. The heat transfer could be declined to a level lower than that of a parallel channel. Hence, the angle of divergence is a critical parameter, which could boost the benefit of using MEPCM suspensions, but it should be selected carefully. The simple convective heat transfer of nanofluids with no phase change has also been investigated in divergent channels [18] and corrugated walls [19].

Very recently, a novel class of encapsulated phase change suspensions, nano-encapsulated phase change materials (NEPCMs) suspensions, has been introduced, and their heat transfer advantages have been reviewed by Liu et al. [20]. The tiny size of nanocapsules allows researchers to synthesize a uniform and stable suspension of NEPCM particles. Hence, the NEPCM-suspensions are an advanced type of hybrid nanofluids, which are promising for various heat transfer applications [21-23]. Dispersed phase change nanoparticles can move with the liquid and contribute to heat transfer by their sensible and latent heat of fusion [24]. Seyf et al. [25] simulated the heat transfer of a NEPCM slurry in a microtube heatsink using a 3D model. They assumed a lumped mass phase change model for the nanoparticles. The authors examined the impact of Reynolds number, particle concentration, and fusion temperature on the cooling behavior of the slurry. Their results showed that a rise in the mass fraction of particles and inlet Reynolds number could improve the Nusselt number and temperature uniformity in the heatsink. Furthermore, the convection heat transfer of NEPCM suspension and slurries have also been addressed in other theoretical works such as backward-step channels [26], micro pin-fin heatsinks [27], and enclosures [28,29], but they have not been investigated for divergent channels.

The literature review shows that the experimental researches on the convective heat transfer and thermal behavior of NEPCM-suspension in mini/microchannels are scarce. Ho et al. [30] examined the heat transfer of NEPCM-suspensions in a minichannel heatsink with a uniform cross-section area. The results showed

that using NECPM-particles could raise the heat transfer rate by about 70% while the index of performance improved by about 45%. Moreover, it was found that the nanoparticles are of interest at small Reynolds numbers since the liquid passes through the channel slowly. Indeed, when the fluid slowly passes through the channel, there is enough time for the heat transfer and interaction between liquid and nanoparticles and heat absorption by latent heat.

As stated, Ho et al. [16,17] explored the forced convection heat transfer of water [16] and MEPCM suspensions [17] in the divergent minichannel heatsinks. Since the liquid has more time to pass the channel, the divergent channel design has a notable advantage over a rectangular minichannel heatsink. Hence, it could be expected that this advantage becomes more evident for the NEPCM suspensions and the contribution of the latent heat. The literature works [16,17] were limited to micro encapsulated phase change suspensions and pure water or a parallel geometry channel [30], while the objective of the present research is to address the convection heat transfer, thermal performance, and pressure drop of nano-encapsulated phase change suspensions in a divergent minichannel heatsink with a divergent angle of 1.36°.

2. Experimental method

2.1. Experimental setup

An experimental setup was constructed to test the forced convective heat transfer of NEPCM-water in a divergent minichannel heatsink. A water-base stable suspension was synthesized to be used as the working fluid. The suspension was introduced to the divergent minichannel to cool the heatsink. The schematic diagram of the experimental setup is depicted in Fig. 1. As seen, a centrifugal pump draws the cold NECPM suspension from a series of cold heat exchangers and pushes it through a controlled temperature heat exchanger. After the control heat exchanger, the suspension passes through the minichannel and absorbs the heat in the form of sensible and latent heat. Since the NEPCM particles shall be solidified, the cold heat exchangers were employed to subcool the suspension. Later, the control heat exchanger was used to adjust the temperature of the working fluid before entering the heatsink. The heat exchangers were immersed in temperature-controlled water tanks. Cotton layers insulated the experimental setup and connecting pipes.

The flow rate of the suspension was measured using a flow meter just before the minichannel test module. A pressure gauge was utilized to record the pressure difference along the minichannel. Two thermocouples were used to monitor the inlet and exit temperatures of the heatsink. Seven thermocouples were used to measure the heatsink temperatures. A block of pure copper with a thermal-conductivity of 401 W/m·K was adopted as the construction material for the heatsink. Eight divergent minichannels were drilled in the copper block to construct the heatsink. The channels were initially etched on the copper block by using the cutting electric discharge method. Then, a computer numerical control machine (CNC) was employed to complete the channel passages. A schematic view of the channel shape and dimensions are illustrated in Fig. 2. The values of the geometric specifications are reported in Table 1. The symbol A_r indicates the height/width (aspect ratio) of a channel, and N denotes the quantity of the etched channels.

The experiment of Ho et al. [31] indicates that the copper is not a proper material to be utilized as the fixture of the heatsink. Copper is highly thermal-conductive, which leads to high heat losses. Thus, Teflon was used as a fixture of the test module. Teflon has good insulation properties, and it is also resistant to high temperatures up to 150 °C. The acrylic glass (PMMA) was chosen for the top cover. Since the acrylic is transparent and thermal resistive, the flow in the channel could also be monitored visually without much heat losses. Two planar elements were used to heat the minichannel uniformly. One of the elements heated the minichannel, and the other element, which was mounted behind the first element, supplies a heat flux to cover the losses at the fixture. Thus, all of the generated heat by the first element will reach the suspension flow. The heating elements are plates of 2 × 50 × 6 mm placed below the minichannel. A DC power supply controlled the required power of the elements. The contacting gap between the plates and the heatsink was filled with thermal paste to reduce the thermal resistance and temperature differences between the element and the heatsink. Moreover, several bolts were used to hold the fixture tight and add pressure between the elements and the heatsink.

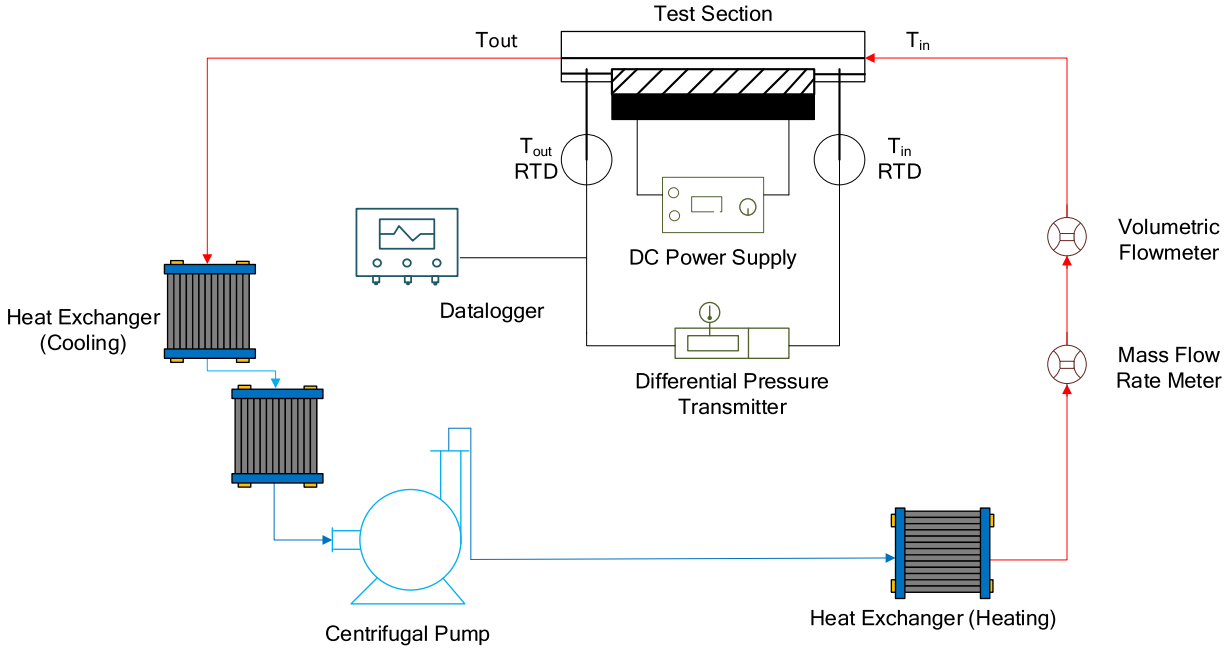

Fig. 1. The test setup and NEPCM suspension loop.

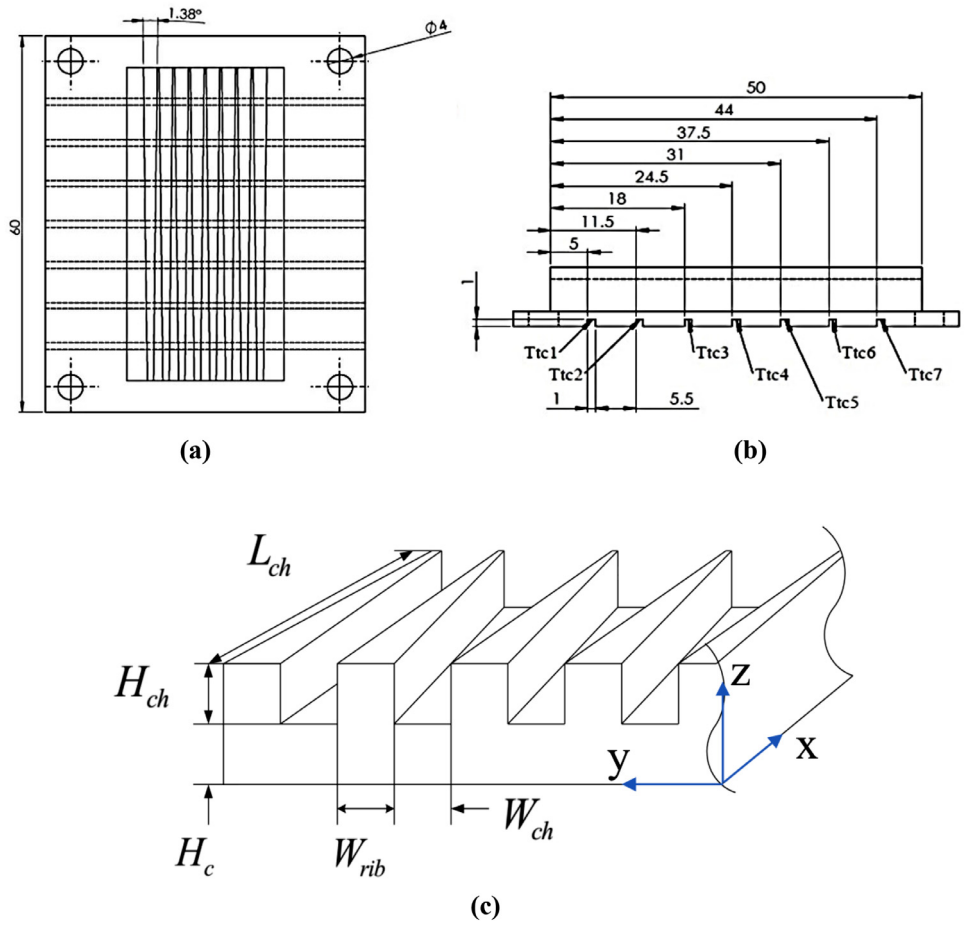

Fig. 2. The geometry of the divergent channel. (a) top view, (b) side view (units are in mm), (c) schematic diagram

Table 1
The size specification of minichannel and the mini heatsink.

Specification	W_{rib}	W_{ch}	H_{ch}	L_{ch}	H_c	A_r	D_H	N
Value (mm)	0.3	2.2	1.5	50	5	0.68	1.6	8

Seven thermocouples were drilled holes below a divergent channel next to the center of the heatsink. The depth of each drilled hole was 5 mm from the bottom of the heatsink. The thermocouples were connected to a data logger, which records the temperatures. The one-dimensional heat conduction approach was employed to evaluate the temperature of the surface channel. The location of the thermocouples is depicted in Fig. 3. The local heat flux can be computed using the surface temperature of the channel. Moreover, the total amount of absorbed heat by the suspension would be the difference between the inlet and outlet enthalpies of the suspension. Tapes and rings were used to waterproof the fixture and heatsink at the bolts and joint locations and reduce the heat losses. The details of the test module are illustrated in Fig. 4.

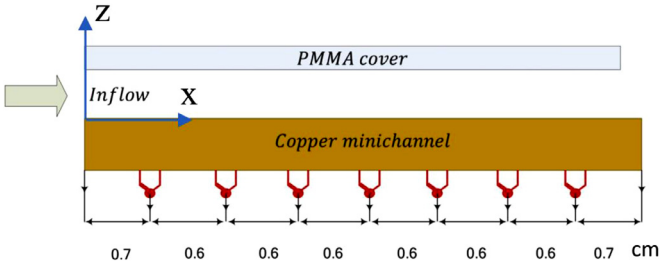

Fig. 3. The placement of the thermocouples below the divergent channel.

2.2. Synthesis of the suspension

The encapsulated particles were synthesized in water using the interfacial condensation polymerization approach. The PCM core was eicosane (the latent heat 247.3J/g), while the formaldehyde was used as a shell. The emulsion was synthesized using the ultrasonication method. More details about the preparation method and Scanning Electron Microscopy (SEM) photo of the nanocapsules have been reported in our previous study [30]. The test results indicate a uniform capsule size of 250-350nm in the water. The thermophysical properties of the NEPCM-suspension were summarized in Table 2. Since the nanoparticles are denser than the water, the overall density of the suspension is higher than the base fluid. Moreover, the concentration of nanoparticles is low, and hence their influence on the thermophysical properties is mini-

Table 2
The measured thermophysical properties of suspension as a function of nanoparticles concentration.

$\omega_{pcm}\omega_{pcm}$ (%)	$\mu \times 10^3$ (N.s/m^2)	k (W/m.K)	c_p (J/kg.K)	P (kg/m^3)
0.0	0.8	0.602	4180	994
0.63	0.97	0.6	4140	996
1.8	1.16	0.59	4080	999
3.8	1.25	0.57	3960	1020

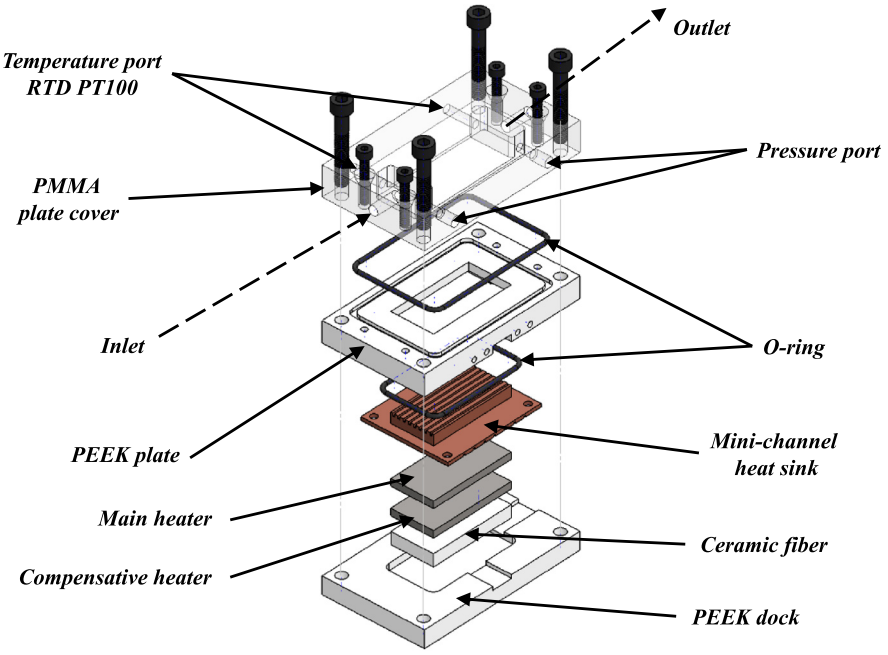

Fig. 4. The test module and the minichannel heatsink.

mal. It is also interesting that suspending the nanoparticles in the hots fluid slightly reduced the overall thermal conductivity of the suspension, but the dynamic viscosity raised. The DSC curves of NEPCMs samples showed that the phase transition temperature of particles during the heating cycle was 34.4°C.

3. Experimental analysis

3.1. The characteristics variables

The Reynolds number shows the strength of the flow in the channel, which was defined using the channel's hydraulic diameter:

$$\mathrm{Re} = \frac{\rho u_m D_H}{\mu} \tag{1}$$

In the above definition, u_m indicates the suspension's average velocity. The average velocity was computed using the volume flow rate and the area of the channel as $\dot{Q}/NA_{ch}$. The hydraulic diameter D_H was computed as D_H=4 × A_{ch}/L_{ch}, where L_{ch} denotes the channel's wet perimeter, and A_{ch} represents the area of the channel cross-section at the inlet of the channel. The volumetric flow through a passage ($\dot{Q}$) was adjusted in the experiment to change the Reynolds number. Since the Reynolds number was computed for one channel, the volume rate of the heatsink was divided by the number of channels, N=8. The size of the channel is in the order of a millimeter; hence, the Reynolds numbers are of the order of hundreds and in the range of 112~940.

As mentioned earlier, the one-dimensional conduction model was used to compute the surface temperature at the interface of the fluid and bottom of the minichannel. Then, the recorded temperatures of the thermocouples at the beneath of the microchannel and the element's heat flux were used to compute the surface temperature. The one-dimensional conduction between the location of the thermocouple and the surface of the channel was written as:

$$T_w = T_{tc} - \frac{q''_{eff} H_c}{k_c} \tag{2}$$

In the above relation, q''_{eff}shows the element heat flux beneath the heatsink. Since the hating power of the element was controlled by DC supply, the heat flux was evaluated as the power divided by the element surface. The symbol H_c denotes the copper thickness between the thermocouple location and the channel surface. The subscripts of *w, tc*, and *c* show the channel surface (wall), the thermocouple, and copper. The demanded pumping power (P) to pass the suspension through the heatsink was computed using the recorded pressure drop between inlet and outlets of the heatsink ΔP multiplied by the flow rate $\dot{Q}$. It should be noted that measuring the pressure drop at the inlet and outlet of the miniature ports of the minichannel is not possible. Thus, following the study of Ho et al. [31], the pressures were measured next to the inlet and outlet ports, and then the pressure drop was corrected by taking account of the pipe losses and expansion and contraction local losses. The inlet's hydraulic-diameter was used for computations. The details of the pressure corrections have been discussed in the studies of Ho et al. [31] as well as [30].

The friction factor was introduced by using pressure drop, the hydraulic diameter of the channel, and the channel length L_{ch} as:

$$f = \frac{1}{2}\frac{D_H}{L_{ch}}\frac{\Delta p}{\rho u_m^2} \tag{3}$$

The mean temperature of the inlet and outlet of the channel and the wall temperature were used to introduce the Nusselt number:

$$\overline{Nu}_{mtd} = \frac{\overline{h}_{mtd} D_H}{k} \tag{4}$$

Here, $\overline{h}_{mtd}$ indicates the average heat transfer coefficient, which was evaluated by using the surface heat flux $\overline{h}_{mtd} = q''_{eff}/(\overline{T}_w - (T_{in} + T_{out})/2)$. The subscripts of *out* and *in* represent inlet and outlet of the minichannel.

In order to judge the effectiveness of using the NEPCM in water compared to the pure water, the convection ratio ($\varepsilon_{\overline{h}_{mtd}}$) was introduced as a ratio of heat transfer coefficient of the NEPCM suspen-

sion to the host fluid:

$$\varepsilon_{\overline{h}_{mtd}} = \frac{\overline{h}_{mtd,nepcm}}{\overline{h}_{mtd,basic}} \tag{5}$$

where the subscripts of *nepm* and *basic* show the NEPCM-suspension and the hots fluid, respectively. An enhanced convection heat transfer due to the presence of NEPCM particles leads to $\varepsilon_{\overline{h}_{mtd}}$ greater than unity, while deterioration of heat transfer leads to a convection ratio smaller than unity.

It should be noted that not only NEPCM particles contribute to heat transfer but also they increase the required pumping power. Therefore, the ratio of the total absorbed energy rate (q_{eff}) to the necessary pump-power (P_m), was introduced by the Coefficient of Performance (*COP*):

$$COP = \frac{q_{eff}}{P_m} \tag{6}$$

Considering the convection ratio ($\varepsilon_{\overline{h}_{mtd}}$) and the pump-power between two states of using NEPCM-water suspension and pure water, the performance index (*FOM*) was introduced as:

$$FOM_{mtd} = \frac{\varepsilon_{\overline{h}_{mtd}}}{(P_{nepcm}/P_{basic})^{\frac{1}{3}}} \tag{7}$$

The Peclet number (*Pe*), Stefan number (Ste^*), and subcooling parameter (Sb_{in}) are defined as below:

$$Pe = \frac{\rho c_p u_m D_H}{k}, Ste^* = \frac{c_p \Delta T_f}{\Delta H}, Sb_{in} = \frac{T_M - T_{in}}{\Delta T_{ref}} \tag{8}$$

In the above equation, the Stefan number represented the comparison of the imposed heating power and the latent heat (ΔH). The parameter Sb_{in} denotes the subcooling parameter. This parameter compares the imposed inlet cooling temperature (T_{in}) with the fusion temperature of NEPCM particles (T_M).

Finally, the dimensionless wall temperature was introduced using the temperature difference between the wall and the inlet temperatures.:

$$\theta_w = \frac{T_w - T_{in}}{\Delta T_{ref}} \tag{9}$$

where the temperature difference was normalized to the relative temperature ($\Delta T_{ref}=q_{eff}/\rho_{bf}C_p\dot{Q}$).

3.2. Uncertainties of the experiment

The uncertainties of the measured values, computed values, and the results of the experiment are summarized in Table 3. These data were used for the error analysis of the findings. The uncertainties of the computed parameters were evaluated using the following relation:

$$erorr(x_1, x_2, \cdots, x_n) = \sqrt{(\Delta x_1 \frac{\partial f}{\partial x_1})^2 + (\Delta x_2 \frac{\partial f}{\partial x_2})^2 + \cdots + (\Delta x_n \frac{\partial f}{\partial x_n})^2} \tag{10}$$

where the *error* indicates a computed error of a variable, which is a function of x_1,x_3, ..., x_n. Here, $\Delta x$is the uncertainty of each measurement.

The range and uncertainty of the computed outcomes are also reported in this table. For example, the reported values of the Nusselt number are within ± 6.8~15.9 (%) uncertainty. The pumping power was also computed within ± 1.2~15.8 uncertainty.

4. Results and discussion

The influence of employing NEPCM-water on the thermal performance of a divergent minichannel with a divergent angle of $\beta = 1.38°$ was examined. The friction factor, the local variation of normal wall temperature, the average Nusselt number, the coefficient of performance, the convection ratio, and the index of performance were addressed for various Reynolds numbers and NEPCM concentrations (ω_{PCM}=0~3.8%). The inlet temperature for all experiments was fixed around 34°C, which is slightly lower than the fusion temperature of 34.4°C.

Fig. 5 illustrates the variation of friction factor for different concentrations of nanoparticles in the divergent channel with $\beta = 1.38°$. This figure exhibits that an increase of the particle concentration surges the friction factor. The straight-line shows the theoretical friction factor for a fully developed flow of a straight channel. For pure water and a low Reynolds number, e.g., $Re_{bf,mean}$=112, the friction factor is slightly smaller than that of the theoretical formula. As the Reynolds number rises, the measured friction factor will be higher than that of the theoretical method. This is since the theoretical formula predicts the friction factor for a fully developed flow, while the flow has not reached a fully developed state in the minichannels of the present experiment. However, due to the change of the geometry and the gradually expanding of the flow channel, the outlet velocity reduces, and the flow condition is close to the fully developed hydrodynamic behavior in a straight channel. It is also found in Fig. 5 that the presence of nanoparticles notably increases the friction factor. Attention to Table 2 indicates that the increase in the concentration of nanoparticles leads to a significant viscosity argumentation. An increase in

Table 3
The uncertainty summary of the measured and computed variables.

Item	Symbol	Range	Uncertainty
Input			
Length of microchannel (mm)	L_{ch}	50mm	± 0.2 mm
Hydraulic diameter(mm)	D_H	1.2mm	± 0.1mm
Current (A)	I	0.65~1.15	± 0.005 Ampere
Concentration (%)	ω_{pcm}	0.63~3.8	± 0.0001%
Voltage (Volt)	V	16~26.2	± 0.05 Volt
Measured			
Temperature (K)	T_{tc}	38.5~86.3	± 0.3 K
Pressure drop (Pa)	Δp	200~6900	± 10 Pa
Volume flow rate (m^3/s)	Q	8.33E-07~7.0E-6	± 0.1~1.1 (%)
Difference of inlet and outlet Temperatures	ΔT	0.35~8.3	± 0.3 K
Result			
FOM	FOM	0.61~1.47	± 5.6~23.8(%)
COP	COP	2224~589094	± 5.5~22.5(%)
Pumping power	P	0.80041E-05~4.7E-3	± 1.2~15.8(%)
Convection ratio	$\varepsilon_{\overline{h}_{mtd}}$	0.7~1.71	± 8.2~25.6(%)
Avg. Nusselt number	$\overline{Nu}_{mtd}$	2.45~9.02	± 6.8~15.9 (%)
Avg. heat transfer coefficient ($W/(m^2K)$)	$\overline{h}_{mtd}$	782~ 4529	± 6.2~15(%)

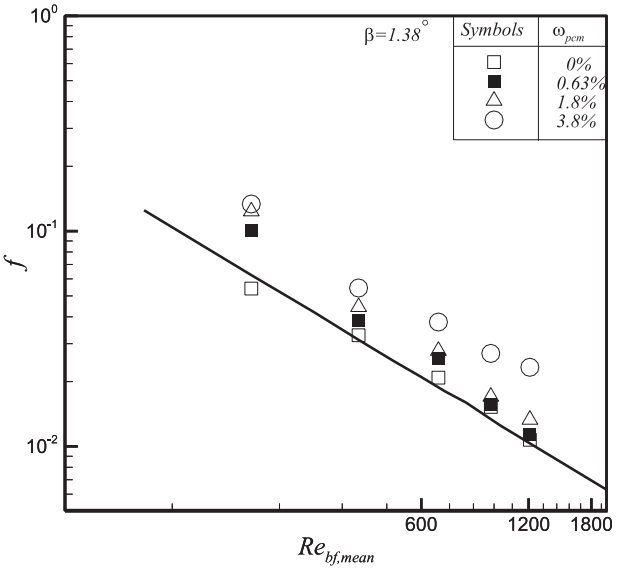

Fig. 5. Relation between friction factor and Reynolds number for various concentrations of NEPCM particles and reference line [32].

the viscosity of liquid results in a higher pressure drop. Hence, the higher the concentration of nanoparticles is, the larger the friction factor is. It is clearly noted from this Fig. 5 that the increase of Reynolds number reduces the friction factor, and the rise in the concentration of nanoparticles boosts the friction factor. Analysis of the recorded data reveals that the growth of the particles' concentration inclines the pressure drop along the channel. Table 2 shows that a 3.8% concentration of particles leads to a 72% surge in the dynamic viscosity.

The distributions of the dimensionless wall temperature along the flow direction of the phase change suspension with different concentrations in the divergent flow channel are presented in Figs. 6 and 7. The results are reported for q_{eff}= 20.6 W (Fig. 6) and q_{eff}=30.2 W (Fig. 7). The outlet temperatures (T_{out}) at various Reynolds numbers were found as 40°C at Re_{bf} = 90, 35.7°C at Re_{bf} = 325, and 34.7 at Re_{bf} = 729 for Fig. 6. The variation of concentration of nanoparticles induces minimum impact on the outlet temperature, and hence, the reported outlet temperatures could be considered for all concentrations. Similarly, the outlet temperature for a higher heating power of 30.2 were found as 42.9°C at Re_{bf} = 90, 36.5°C at Re_{bf} = 325, and 35.1 at Re_{bf} = 729. Here, x^+ denotes the local length along the channel in flow direction.

As seen, when the flow rate is low, the working fluid should absorb a significant amount of heat until it reaches the outlet. Thus, in this case, the liquid temperature is fairly higher than the fusion temperature of nanoparticles. As a result, a uniform full melt of particles could be expected. In the case of a moderate flow rate, the working fluid is only a few degrees higher than the fusion temperature of nanoparticles. Thus, it could be expected that some of the nanoparticles do not melt completely. This situation could get worsen for larger Reynolds numbers and high flow rates. The results showed that the outlet temperature was further increased for higher heat flux. In this case, the nanoparticles could better contribute to the heat transfer due to a higher temperature difference between the liquid and particles' fusion temperature. As a general conclusion, the increase of the heat flux or the reduction of flow rate would boost the temperature growth of liquid through the channel and will intensify the phase change heat transfer of nanoparticles.

Regardless of the heating power, employing the nanoparticles reduces the wall temperature for the cases with small Reynolds numbers significantly. The increase of concentration of nanoparticles boosts the wall temperature reduction. At middle Reynolds-numbers, there is also a decrease in the wall temperature, but this advantage is only notable at high concentrations of nanoparticles. At high Reynolds numbers, using NEPCM particle lose its advantage. In the case of high heating power (30.2 W), the wall temperature slightly grows. The presence of 0.63% nanoparticles deteriorates the heat transfer at high heat power of (20.6W) and high Reynolds numbers, but NEPMCs could still be advantageous in the lower heating power of 30.2W. As a general conclusion, using phase change nanoparticles at low Reynolds numbers notably enhances the convection rate and declines the wall temperature. At the middle Reynolds number, a very good wall temperature reduction could be observed. However, solely high concentrations of nanoparticles could be beneficial at high Reynolds numbers. As the heating power increases, high concentrations of nanoparticles are required to maintain the advantage of using NEPCMs.

Fig. 8 shows the average Nusselt number under different heating power and the nanoparticle concentration for the divergent minichannel. In various experimental conditions, it can be seen that the Nusselt number rises with an increase of the Reynolds number for the middle and low Reynolds numbers ($Re_{bf,mean}$=112~403). The incline of the average Nusselt number follows a similar trend as the experimental results of the pure water. However, the presence of NEPCMs with a concentration of 0.63%

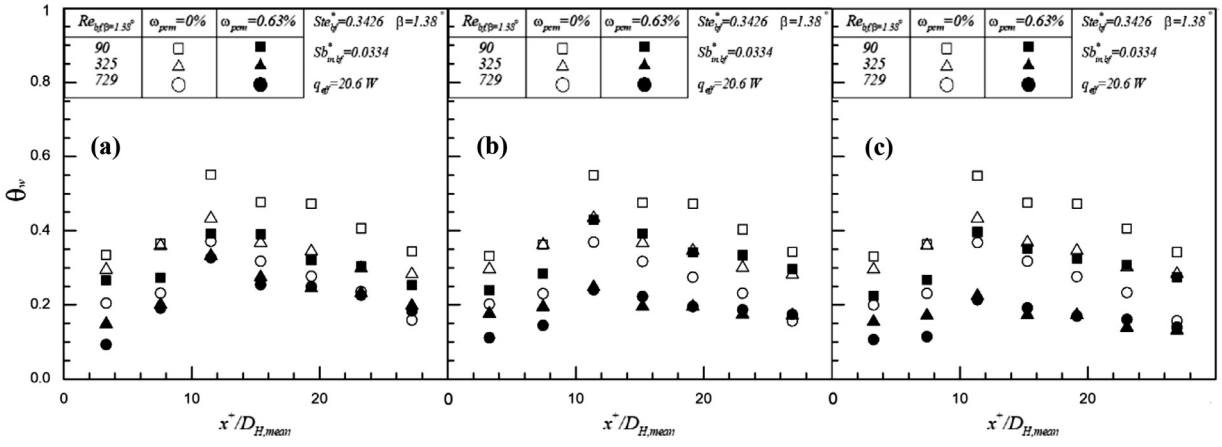

Fig. 6. Variation of normal wall temperature along the channel when 20.6 W as a function of the concentration of nanoparticles; (a) concentration of 0.63%, (b) concentration of 1.8%, and (c) concentration of 3.8%.

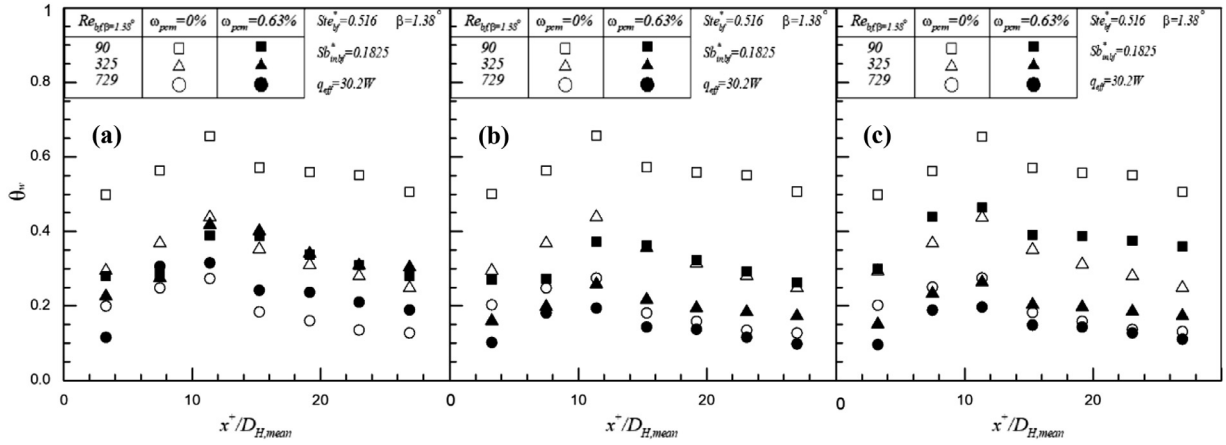

Fig. 7. Variation of normal wall temperature along the channel when 30.2 W as a function of the concentration of nanoparticles; (a) concentration of 0.63%, (b) concentration of 1.8%, and (c) concentration of 3.8%.

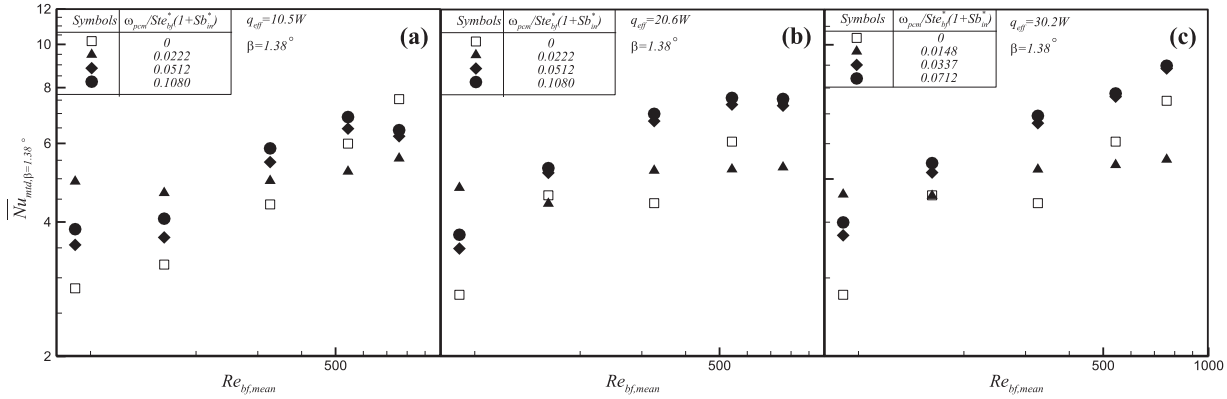

Fig. 8. The impact of Reynolds number and heat capacity ratio on the average Nusselt number ($\overline{Nu}_{mtd}$) at different heating powers; (a) 10.5 W, (b) 20.6 W, and (c) 30.2 W.

deteriorates the heat transfer in the case of low hating power, 10.5 W, and at a slightly higher Reynolds number ($Re_{bf,mean}$=672). The phase change suspension with different concentrations has a turning point at a higher Reynolds number ($Re_{bf,mean}$=940). Using NEPCMs at a high Reynolds number is not beneficial regardless of the concentration of the nanoparticles. This turning point shifts to lower Reynolds numbers as the heating power increases to 20.6 W and 30.2 W. It is speculated that the generation of these turning points is related to whether a phase change material can absorb the channel heat in the form of latent heat. Before this critical Reynolds number, the phase change particles could effectively absorb the heat, so the heat transfer was dominated by latent heat. After this critical Reynolds number, the heat transfer is dominated by sensible heat. Besides, the high Reynolds number part is also consistent with the dimensionless wall temperature distribution. The highest Nusselt number corresponds to the maximum Reynolds number and the largest magnitude of $\omega_{pcm}/(Ste^* \times (1+Sb_{in}{}^*)$.

As shown in Fig. 9, the highest heat transfer ratio appears in the experimental condition of Reynolds number 112, when the actual latent heat sensible heat ratio is 0.0712. This figure, in agreement with the previous observations, shows that the general advantage of using nanoparticles is toward a high concentration of nanoparticles and low flow rates (small Reynolds numbers). It is worth noting that at the lowest Reynolds number, the distribution of heat transfer ratio does not follow the concentration change and has a certain trend. It can be seen that when $(\omega_{pcm}/(Ste^* \times (1+Sb_{in}{}^*) = 0.512$ (1.8%), the heat transfer ratio is the lowest, followed by the actual latent heat sensible heat ratio at 0.0712 (0.63%) and 0.1080 (3.8%). It is speculated that at the lowest Reynolds number, the benefit of convection heat transfer is quite low, and there is a competition between the decrease of sensible heat due to the presence of nanoparticles and the enhancement of latent heat capacity. The experimental results show that the time that the suspension passes through the channel should be extended so the phase change capsules could better absorb heat (meaning low flow rate). Moreover, it is also necessary to increase the heat absorption rate (control of heating power) to achieve the best heat transfer ratio. In addition, physical properties must be considered. For instance, the increase of concentration may drastically increase the viscosity, which diminishes the convection heat transfer and deteriorate the overall heat transfer rate for small Reynolds numbers. Besides, in the low concentration part, consistent with the dimensionless wall temperature, the heat transfer ratio is less than unity in the high Reynolds number region. The maximum heat transfer ratio takes place at Re_{bf}=112, and the actual latent heat sensible heat ratio of 0.0712, which reaches 82%.

The relationship between the performance index (*FOM*) and the Reynolds number at various values of heating power and concentrations is shown in Fig. 10. The trend is similar to the heat transfer ratio since *FOM* is indeed a combination of the heat transfer ratio and pump power. Therefore, it is consistent with the trend of the heat transfer ratio, but the increase of the concentration of nanoparticles gradually increases the viscosity of the suspension and, eventually, the required pump power. This figure shows that the *FOM* is generally higher than unity at low to middle Reynolds numbers and low to middle values of heating-powers. The *FOM*

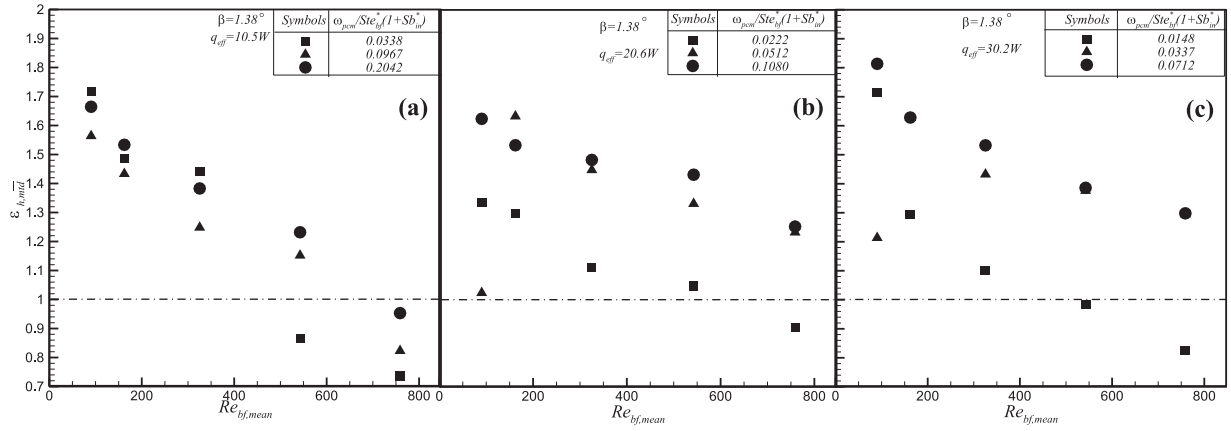

Fig. 9. The impact of Reynolds number and heat capacity ratio on the heat convection ratio at various heating powers; (a) 10.5 W, (b) 20.6 W, and (c) 30.2 W

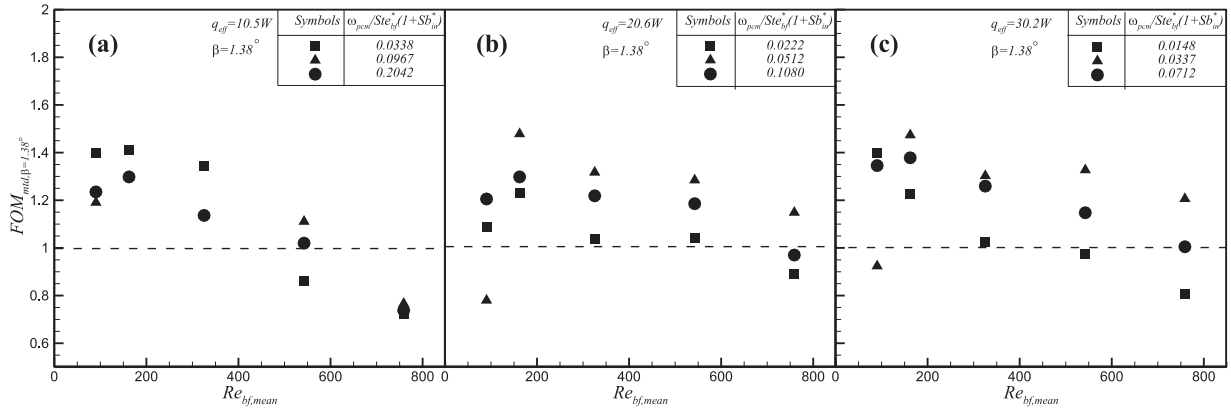

Fig. 10. The impact of Reynolds number and heat capacity ratio on the performance index (FOM_{mtd}) at various heating powers; (a) 10.5 W, (b) 20.6 W, and (c) 30.2 W.

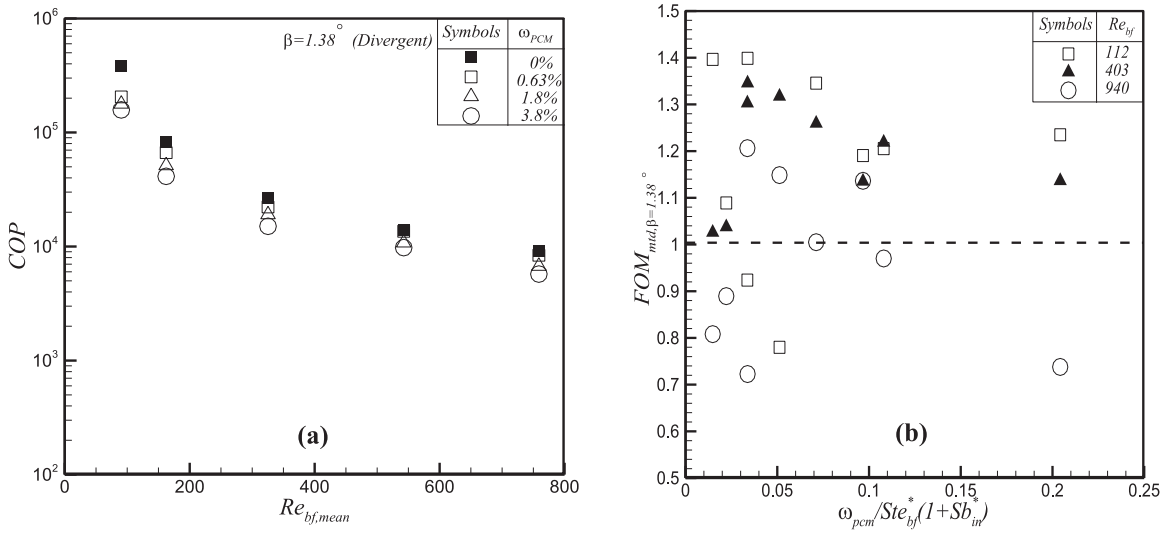

Fig. 11. The overall variation of the coefficient of performance and index of performance as a function of Reynolds number when q_{eff} = 30.2 W; (a) *COP*, and (b) FOM_{mtd}.

drops to below unity at high Reynolds numbers and high heating powers.

Fig. 11(a) depicts the relationship between *COP* and Reynolds number. This figure was plotted when the heating power was constant at q_{eff}=30.2 W, and the flow rate was increased gradually. As seen, the pumping power drastically increases by the increase of the concentration of nanoparticles, but the heat transfer rate increases moderately, and in some cases, it could deteriorate. Thus, it can be seen that *COP* is inversely proportional to the concentration of NEPCM particles. Fig. 11(b) provides a comprehensive map for the index of performance of the suspension at various Reynolds numbers and latent heat sensible heat ratios. This figure illustrates the *FOM* for various values of latent heat sensible heat ratio ($\omega_{pcm}/[Ste^* \times (1+Sb_{in}{}^*)]$). Interestingly this figure demonstrates that using nanoparticles at a moderate Reynolds numbers of Re=403 leads to an increase of heat transfer rate and an ac-

ceptable increase of pumping power. So, the *FOM* is above unity. The benefit of using nanoparticles at higher Reynolds numbers depends on the latent heat sensible heat ratio.

5. Conclusion

The convective heat transfer of a nano-encapsulated phase-change suspension in a divergent channel mini heatsink was addressed experimentally. The heatsink was made of copper with eight divergent flow passages. The subcooled NEPCM-suspension, as the working fluid, was circulated in the heated minichannel. The phase change nanoparticles move with the water in the channel and melt. During their melting process, they and absorb the channel's heat in the form of latent heat. Various characteristic parameters such as Nusselt number, temperature variation at the channel wall, convection heat transfer ratio, coefficient of performance, and the index of performance were investigated. The outcomes indicate that the advantage of using the NEPCM suspension depends on the flow Reynolds number, concentration of nanoparticles, and heating power. The main finding of the present research can be summarized as follows.

(1) The presence of NEPCM particles leads to a notable pressure drop across the channel due to the augmentation of dynamic viscosity. However, when the Reynolds number is low, they can significantly contribute to the heat transfer and reduce the channel temperature and boost the Nusselt number.
(2) The maximum heat transfer ratio could be detected a low Reynolds number of 112, and the concentration of 3.8% and maximum element power $q_{eff} = 30.2$ W. The temperature differences are quite significant in the divergent channel for this case. Since at a small Reynolds number, the suspension passes through the channel slowly, the nanoparticles could effectively melt and absorb the element's heat. This case corresponds to 82% heat transfer enhancement in the channel compared to the pure fluid.
(3) Considering the pumping power and heat transfer, the moderate Reynolds number of Re=403 could result in a performance of index higher than unity for all concentrations of nanoparticles and heating powers. In the case of high Reynolds numbers, the suspension passes through the divergent channel too quickly, and hence, the nanoparticles cannot properly absorb the heat and melt. In such a case, the heat transfer mostly occurs by the sensible heat of the suspension. Thus, using NEPCM particles could not be advantageous unless for high concentrations.

Declaration of Competing Interest

None

CRediT authorship contribution statement

C.J. Ho: Conceptualization, Supervision, Validation, Data curation. **Yen-Chung Liu:** Investigation. **Tien-Fu Yang:** Validation, Data curation, Writing - original draft, Writing - review & editing. **Mohammad Ghalambaz:** Writing - original draft, Writing - review & editing. **Wei-Mon Yan:** Validation, Data curation, Writing - original draft, Writing - review & editing.

Acknowledgments

The financial support from Ministry of Science and Technology, Taiwan, under grant number MOST 106-2221-E-027-103 is acknowledged. The authors also appreciate the financial support from the "Research Center of Energy Conservation for New Generation of Residential, Commercial, and Industrial Sectors" from The Featured Areas Research Center Program within the framework of the Higher Education Sprout Project by the Ministry of Education (MOE) in Taiwan.

References

[1] M.A. Sheremet, N. Bondareva, F.-Y. Zhao, The brick thermal performance improvement using phase change materials, Journal of Applied and Computational Mechanics (2020).
[2] H.M. Sadeghi, M. Babayan, A. Chamkha, Investigation of using multi-layer PCMs in the tubular heat exchanger with periodic heat transfer boundary condition, International Journal of Heat and Mass Transfer 147 (2020) 118970.
[3] S. Kumar, A. Kumar, A.D. Kothiyal, M.S. Bisht, A review of flow and heat transfer behaviour of nanofluids in micro channel heat sinks, Thermal Science and Engineering Progress 8 (2018) 477–493.
[4] N.A.C. Sidik, M.N.A.W. Muhamad, W.M.A.A. Japar, Z.A. Rasid, An overview of passive techniques for heat transfer augmentation in microchannel heat sink, International Communications in Heat and Mass Transfer 88 (2017) 74–83.
[5] B. Gireesha, B. Mahanthesh, A.J. Chamkha, Entropy generation analysis of magneto-nanoliquids embedded with aluminium and titanium alloy nanoparticles in microchannel with partial slips and convective conditions, International Journal of Numerical Methods for Heat & Fluid Flow (2018).
[6] Y. Ma, A. Shahsavar, P. Talebizadehsardari, Two-phase mixture simulation of the effect of fin arrangement on first and second law performance of a bifurcation microchannels heatsink operated with biologically prepared water-Ag nanofluid, International Communications in Heat and Mass Transfer 114 (2020) 104554.
[7] S. Sindhu, B. Gireesha, Entropy generation analysis of hybrid nanofluid in a microchannel with slip flow, convective boundary and nonlinear heat flux, International Journal of Numerical Methods for Heat & Fluid Flow (2020).
[8] A.A. Hussien, M.Z. Abdullah, A.-N. Moh'd A, Single-phase heat transfer enhancement in micro/minichannels using nanofluids: theory and applications, Applied energy 164 (2016) 733–755.
[9] M. Delgado, A. Lázaro, J. Mazo, B. Zalba, Review on phase change material emulsions and microencapsulated phase change material slurries: materials, heat transfer studies and applications, Renewable and Sustainable Energy Reviews 16 (1) (2012) 253–273.
[10] L. Chen, T. Wang, Y. Zhao, X.-R. Zhang, Characterization of thermal and hydrodynamic properties for microencapsulated phase change slurry (MPCS), Energy conversion and management 79 (2014) 317–333.
[11] Y. Wang, Z. Chen, X. Ling, An experimental study of the latent functionally thermal fluid with micro-encapsulated phase change material particles flowing in microchannels, Applied Thermal Engineering 105 (2016) 209–216.
[12] R. Sabbah, M.M. Farid, S. Al-Hallaj, Micro-channel heat sink with slurry of water with micro-encapsulated phase change material: 3D-numerical study, Applied Thermal Engineering 29 (2-3) (2009) 445–454.
[13] L. Liu, G. Alva, Y. Jia, X. Huang, G. Fang, Dynamic thermal characteristics analysis of microencapsulated phase change suspensions flowing through rectangular mini-channels for thermal energy storage, Energy and Buildings 134 (2017) 37–51.
[14] M.M. Farid, S. Al-Hallaj, Microchannel heat exchanger with micro-encapsulated phase change material for high flux cooling, Google Patents (2012).
[15] X.J. Wang, Liquid coolant with microencapsulated phase change materials for automotive batteries, Google Patents (2014).
[16] C. Ho, P.C. Chang, W.M. Yan, P. Amani, Thermal and hydrodynamic characteristics of divergent rectangular minichannel heat sinks, International Journal of Heat and Mass Transfer 122 (2018) 264–274.
[17] C. Ho, P.C. Chang, W.M. Yan, M. Amani, Comparative study on thermal performance of MEPCM suspensions in parallel and divergent minichannel heat sinks, International Communications in Heat and Mass Transfer 94 (2018) 96–105.
[18] M. Hatami, L. Sun, D. Jing, H. Günerhan, P.K. Kameswaran, Rotating Cylinder Turbulator Effect on The Heat Transfer of a Nanofluid Flow in a Wavy Divergent Channel, Journal of Applied and Computational Mechanics (2020).
[19] A. Begag, S. Rachid, H.F. Oztop, A. Said, Numerical study on heat transfer and pressure drop in a mini-channel with corrugated walls, Journal of Applied and Computational Mechanics (2020).
[20] C. Liu, Z. Rao, J. Zhao, Y. Huo, Y. Li, Review on nanoencapsulated phase change materials: preparation, characterization and heat transfer enhancement, Nano Energy 13 (2015) 814–826.
[21] S. Barlak, O.N. Sara, A. Karaipekli, S. Yapıcı, Thermal conductivity and viscosity of nanofluids having nanoencapsulated phase change material, Nanoscale and Microscale Thermophysical Engineering 20 (2) (2016) 85–96.
[22] H. Yuan, H. Bai, Y. Wang, Preparation and Characterization of Stearic Acid/SiO 2 Nano-encapsulated Phase Change Materials via Sol-gel Method, in: Energy Technology 2016, Springer, 2016, pp. 99–106.
[23] M.S. Ghoghaei, A. Mahmoudian, O. Mohammadi, M.B. Shafii, H. Jafari Mosleh, M. Zandieh, M.H. Ahmadi, A review on the applications of micro-/nano-encapsulated phase change material slurry in heat transfer and thermal storage systems, Journal of Thermal Analysis and Calorimetry (2020) 1–24.
[24] M. Ghalambaz, A.J. Chamkha, D. Wen, Natural convective flow and heat transfer of Nano-Encapsulated Phase Change Materials (NEPCMs) in a cavity, International Journal of Heat and Mass Transfer 138 (2019) 738–749.

[25] H.R. Seyf, Z. Zhou, H. Ma, Y. Zhang, Three dimensional numerical study of heat-transfer enhancement by nano-encapsulated phase change material slurry in microtube heat sinks with tangential impingement, International journal of heat and mass transfer 56 (1-2) (2013) 561–573.
[26] H. Lu, H.R. Seyf, Y. Zhang, H. Ma, Heat transfer enhancement of backward-facing step flow by using nano-encapsulated phase change material slurry, Numerical Heat Transfer, Part A: Applications 67 (4) (2015) 381–400.
[27] B. Rajabifar, H.R. Seyf, Y. Zhang, S.K. Khanna, Flow and heat transfer in micro pin fin heat sinks with nano-encapsulated phase change materials, Journal of Heat Transfer 138 (6) (2016).
[28] M. Ghalambaz, S. Mehryan, I. Zahmatkesh, A. Chamkha, Free convection heat transfer analysis of a suspension of nano–encapsulated phase change materials (NEPCMs) in an inclined porous cavity, International Journal of Thermal Sciences 157 (2020) 106503.
[29] S. Mehryan, M. Ghalambaz, L.S. Gargari, A. Hajjar, M. Sheremet, Natural convection flow of a suspension containing nano-encapsulated phase change particles in an eccentric annulus, Journal of Energy Storage 28 (2020) 101236.
[30] C. Ho, Y.C. Liu, M. Ghalambaz, W.M. Yan, Forced convection heat transfer of Nano-Encapsulated Phase Change Material (NEPCM) suspension in a mini-channel heatsink, International Journal of Heat and Mass Transfer 155 (2020) 119858.
[31] C.J. Ho, L.C. Wei, Z.W. Li, An experimental investigation of forced convective cooling performance of a microchannel heat sink with Al2O3/water nanofluid, Applied Thermal Engineering 30 (2-3) (2010) 96–103.
[32] W.C. Cheng, Heat transfer experiment on forced convection performance of water-based suspensions of nanoparticles and/or MEPCM particles in a minichannel heatsink Master thesis, National Cheng Kung University, Taiwan, 2009.